



US 20070167779A1

(19) **United States**

(12) **Patent Application Publication**

Kim et al.

(10) **Pub. No.: US 2007/0167779 A1**

(43) **Pub. Date: Jul. 19, 2007**

(54) **ULTRASOUND IMAGING SYSTEM FOR EXTRACTING VOLUME OF AN OBJECT FROM AN ULTRASOUND IMAGE AND METHOD FOR THE SAME**

(75) Inventors: **Nam Chul Kim**, Daegu (KR); **Jong Hwan Oh**, Gumi-si (KR); **Sang Hyun Kim**, Busan (KR); **Jong In Kwak**, Daegu (KR); **Chi Young Ahn**, Seoul (KR)

Correspondence Address:

**OBLON, SPIVAK, MCCLELLAND, MAIER & NEUSTADT, P.C.**  
**1940 DUKE STREET**  
**ALEXANDRIA, VA 22314 (US)**

(73) Assignee: **Medison Co., Ltd.**, Hongchun-gu (KR)

(21) Appl. No.: **11/539,460**

(22) Filed: **Oct. 6, 2006**

(30) **Foreign Application Priority Data**

Oct. 7, 2005 (KR) ..... 10-2005-0094318

**Publication Classification**

(51) **Int. Cl.**  
**A61B 8/00** (2006.01)  
(52) **U.S. Cl.** ..... **600/443**

(57) **ABSTRACT**

The present invention provides an ultrasound imaging system for forming 3D volume data of a target object, including a three-dimensional (3D) image providing unit for providing a 3D ultrasound image; a pre-processing unit for forming a number of two-dimensional (2D) images from the 3D ultrasound image and normalizing the 2D images to form normalized 2D images; an edge extraction unit for forming wavelet-transformed images of the normalized 2D images at a number of scales, the edge extraction unit further being configured to form edge images by averaging the wavelet-transformed images at a number of scales and threshold the edge images; a control point determining unit for determining control points by using a support vector machine (SVM) based on the normalized 2D images, the wavelet-transformed images and the thresholded edge images; and a rendering unit for forming 3D volume data of the target object by 3D rendering based on the control points.

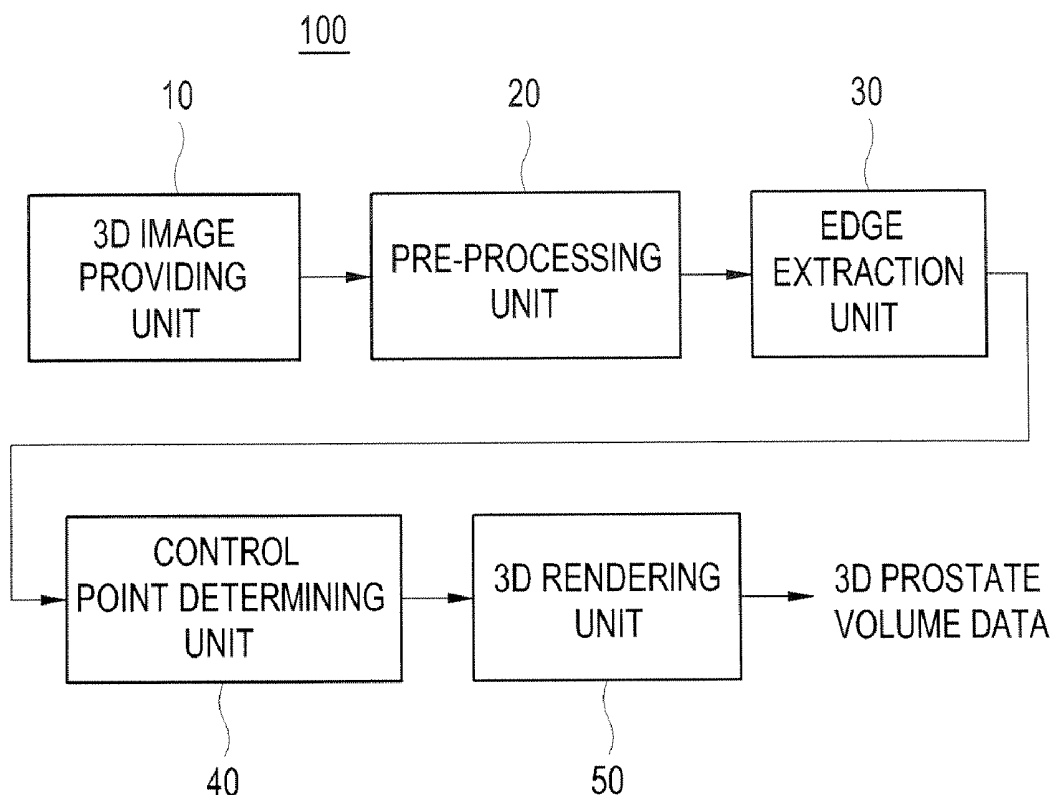


FIG. 1

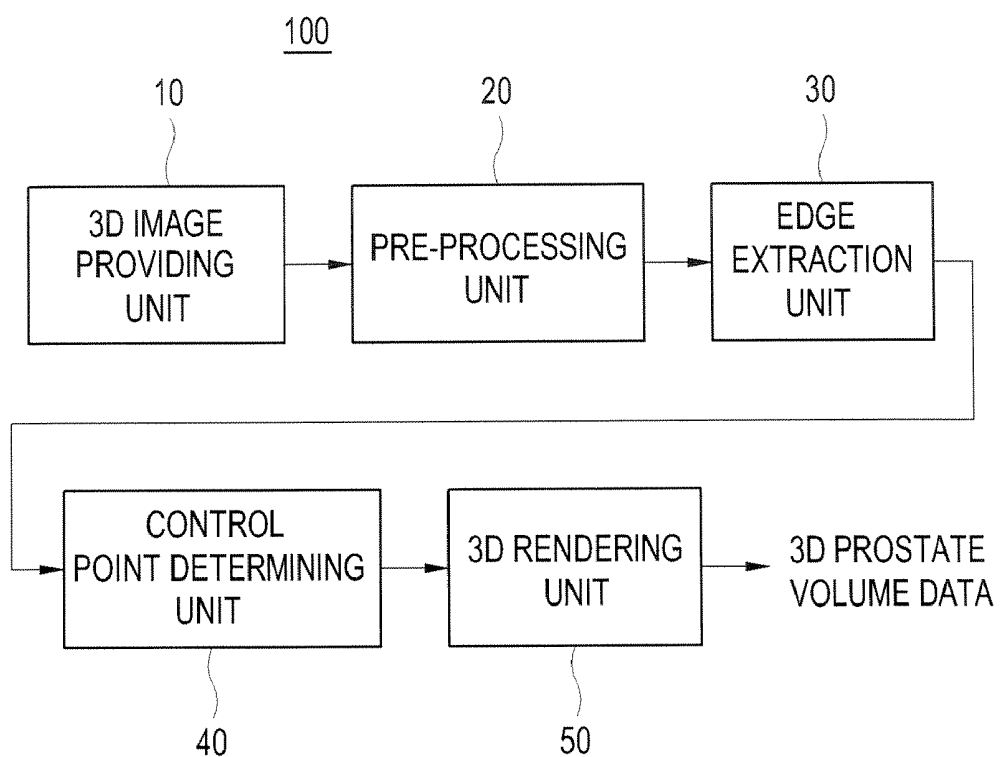


FIG. 2

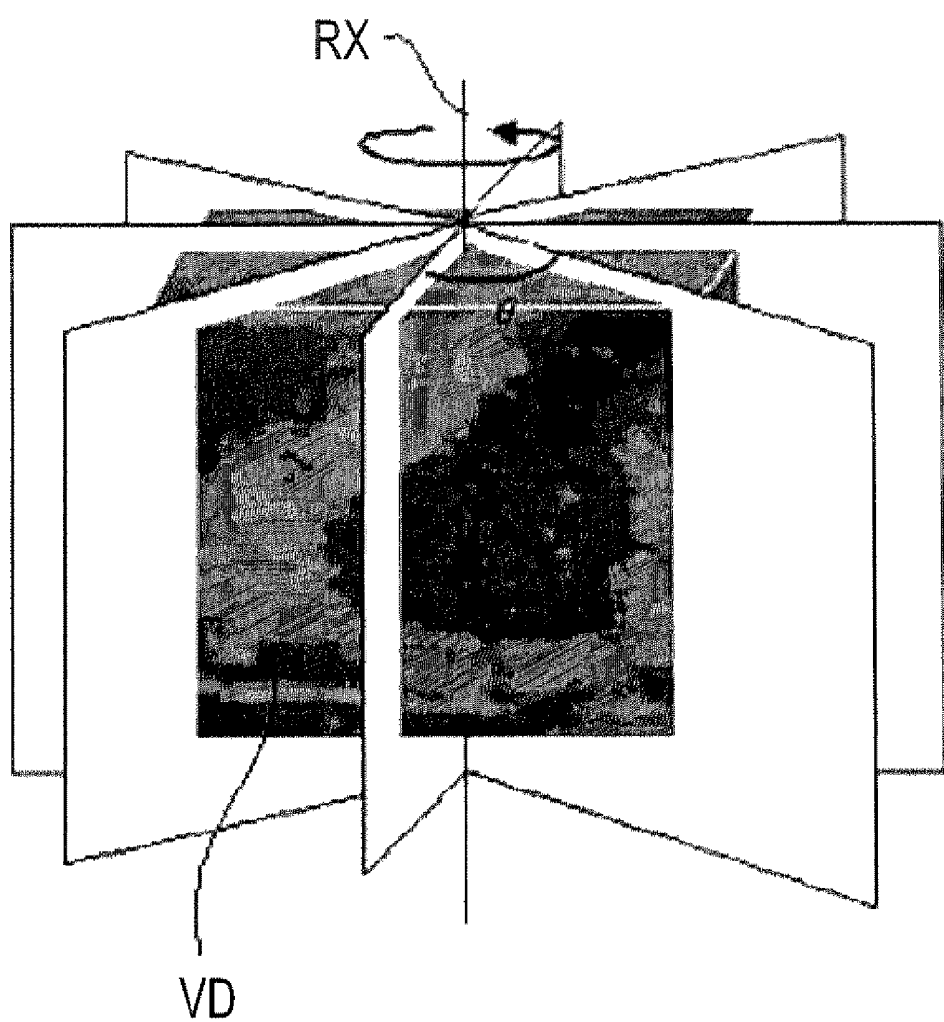


FIG. 3A

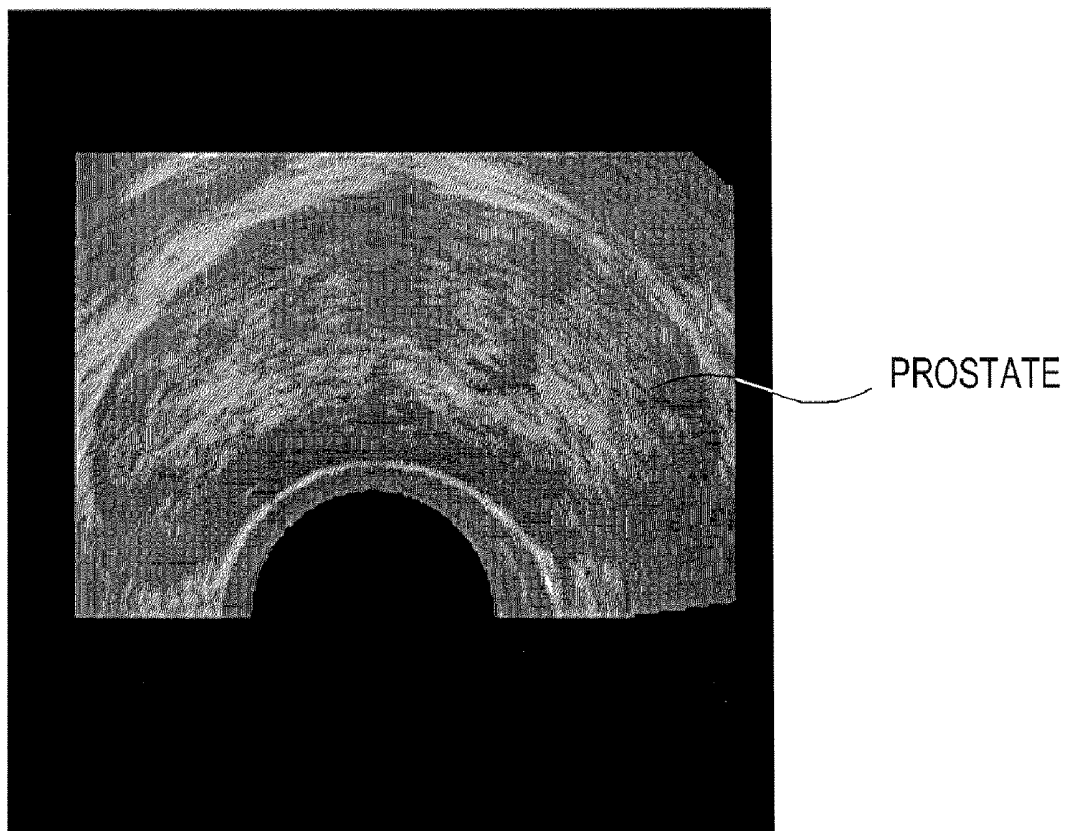


FIG. 3B

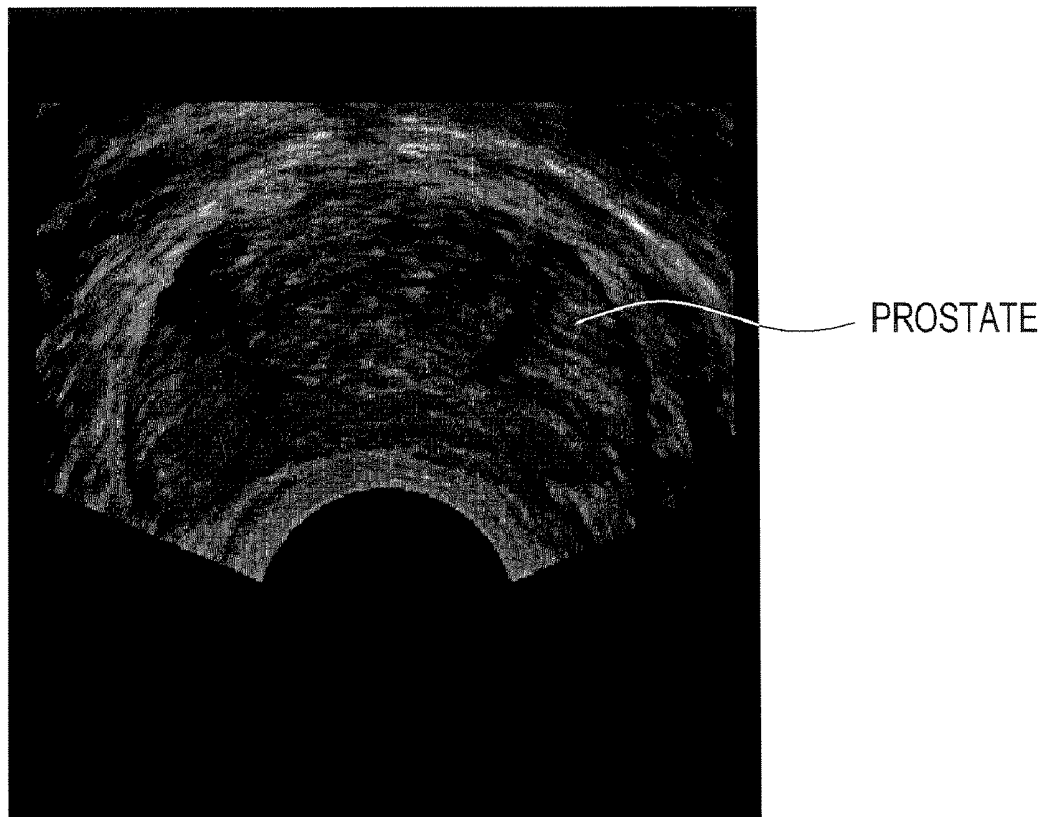


FIG. 4A

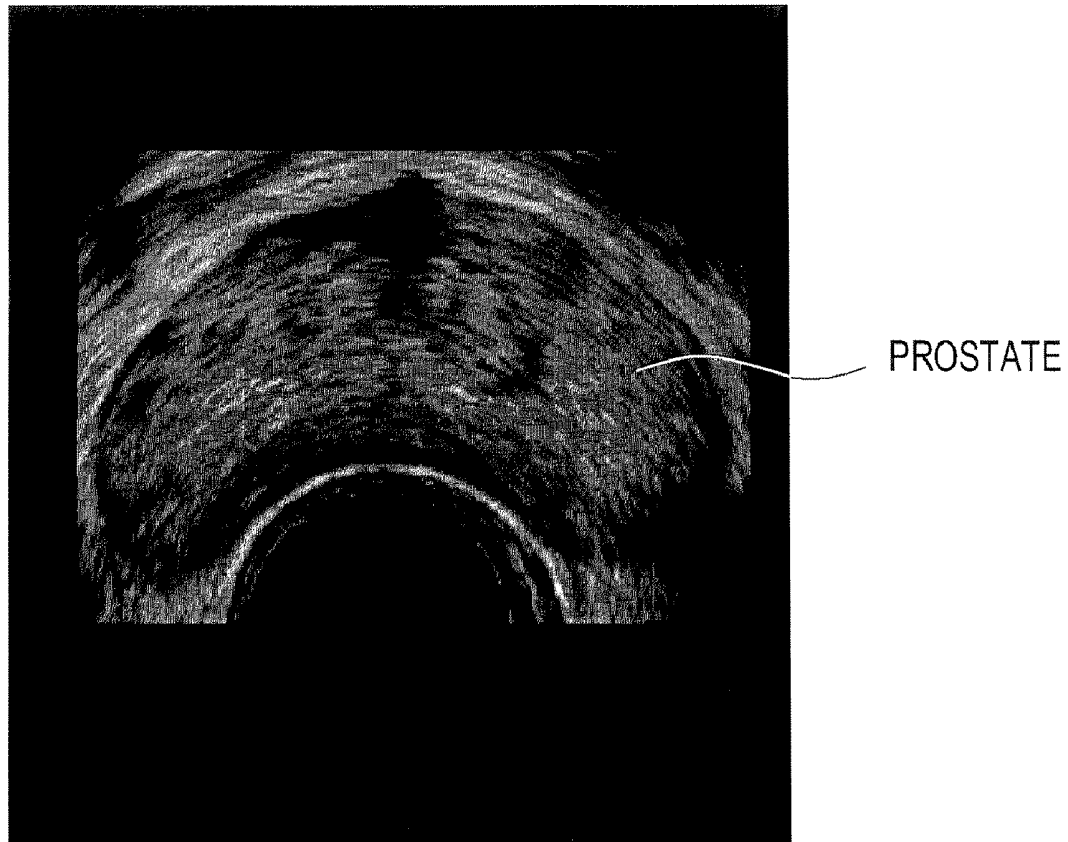


FIG. 4B

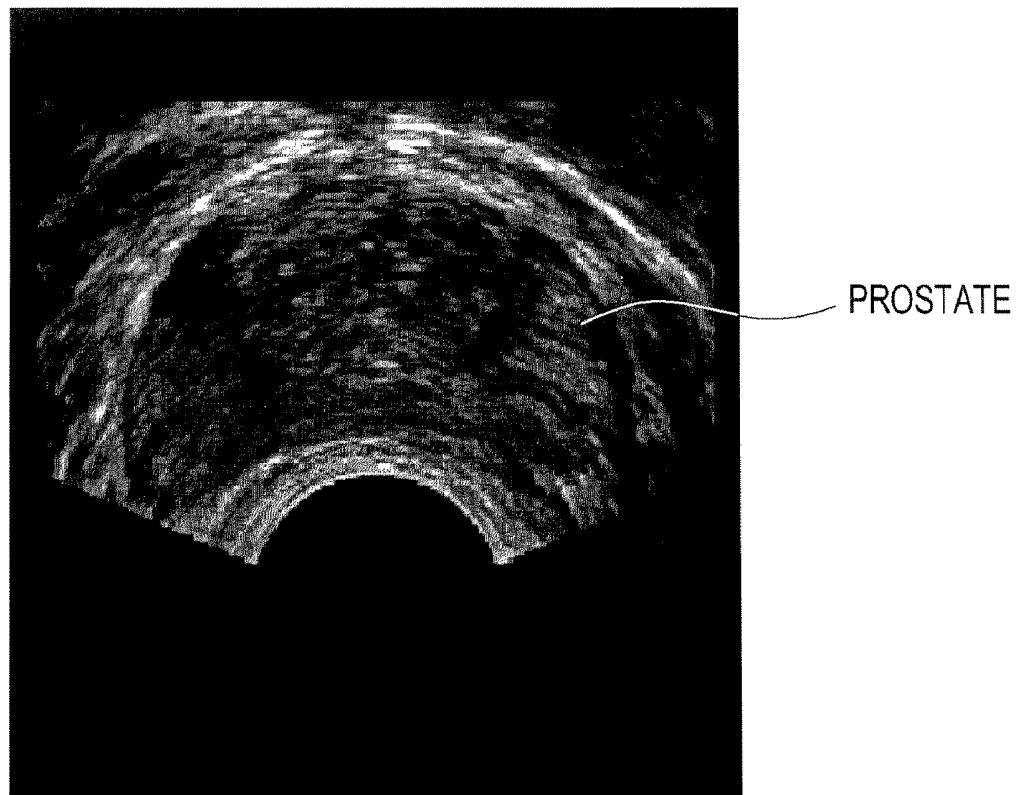


FIG. 5

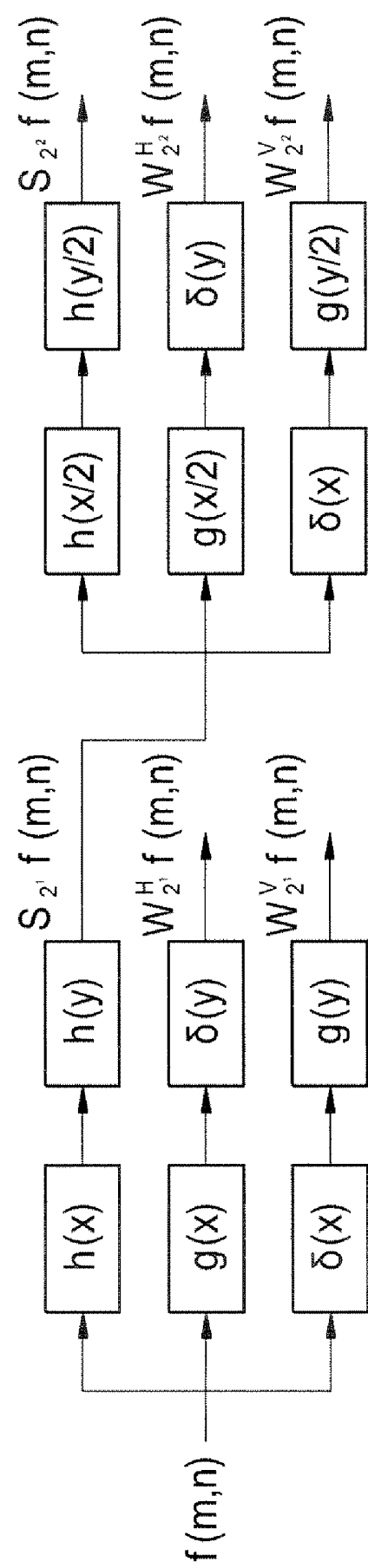


FIG. 6A

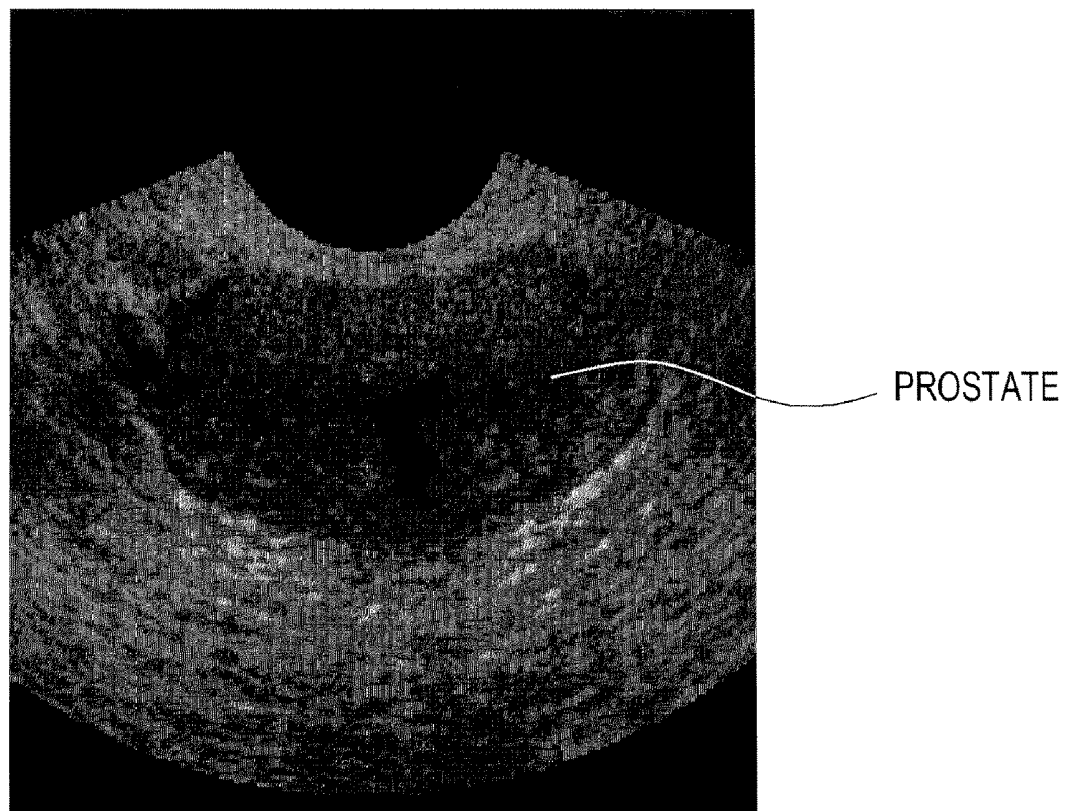


FIG. 6B

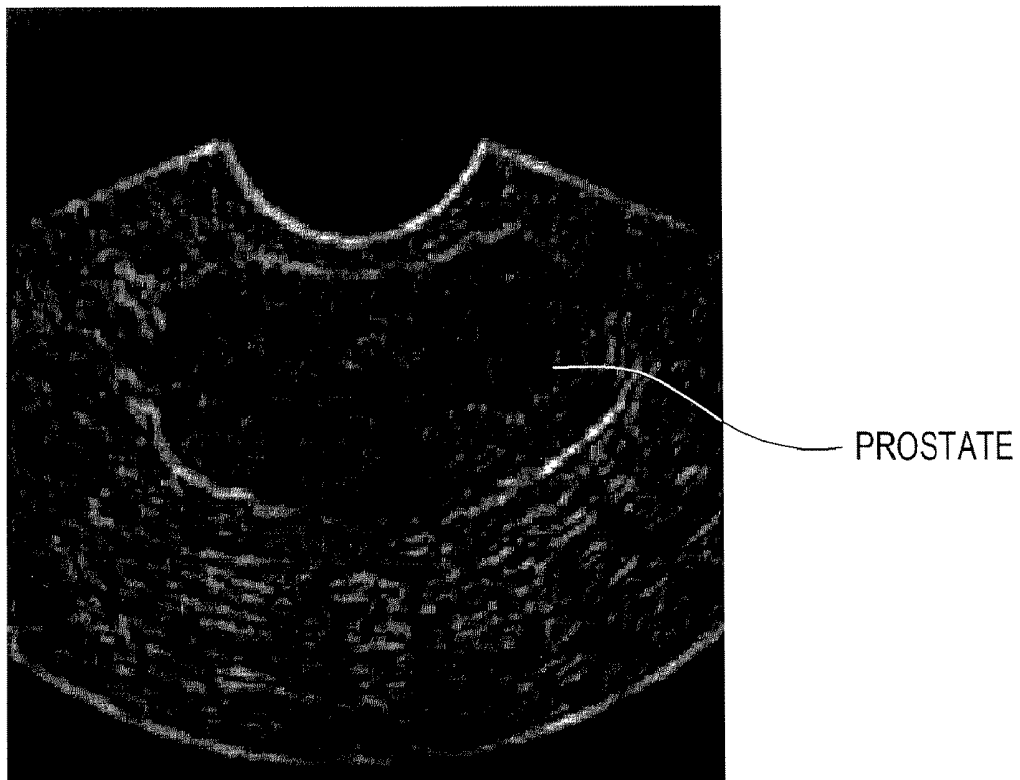


FIG. 6C

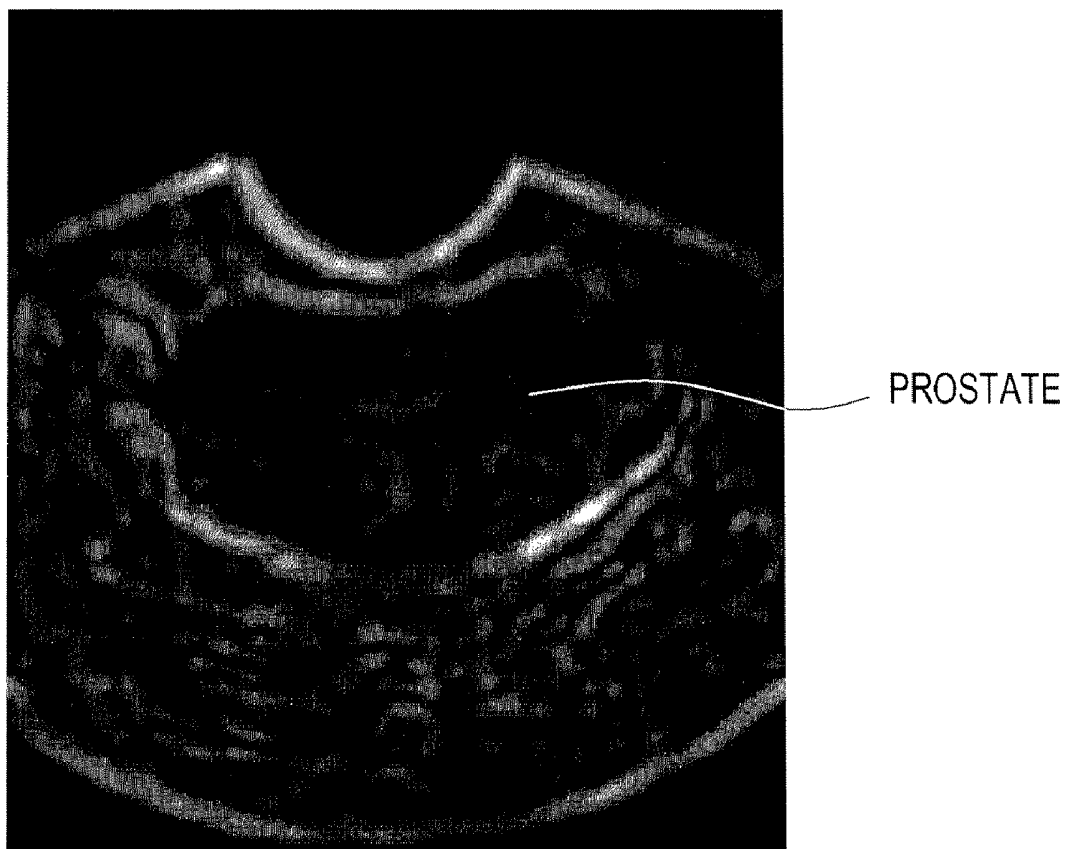


FIG. 6D

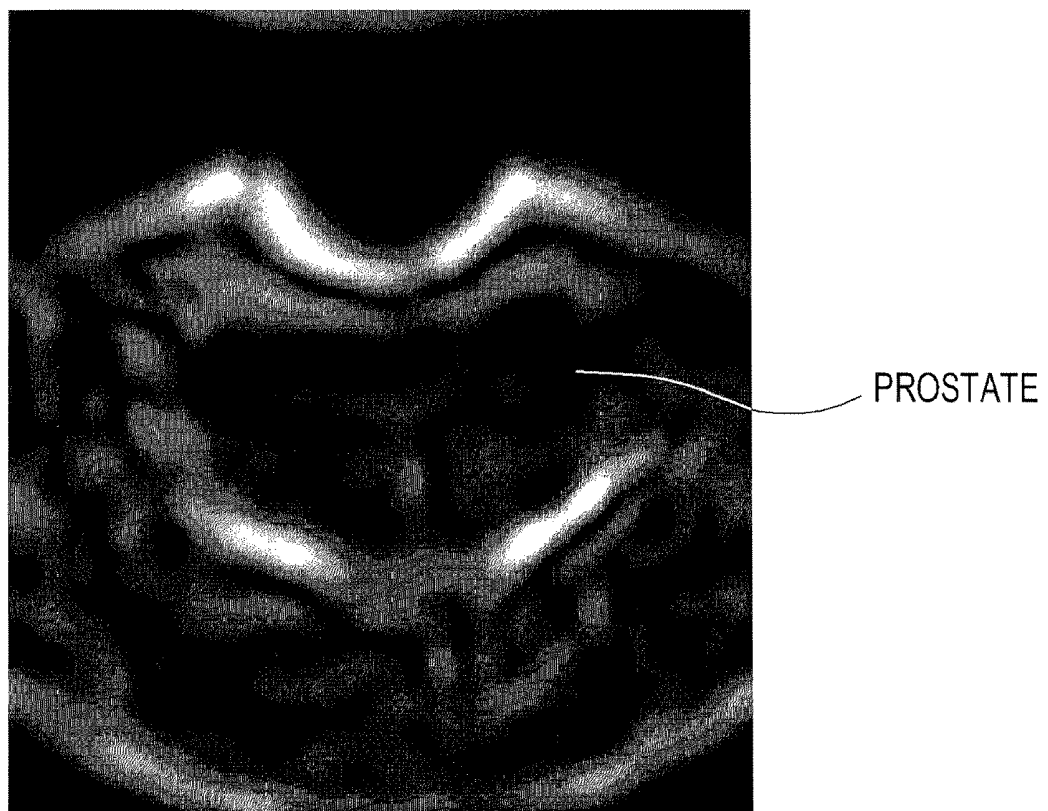


FIG. 7A

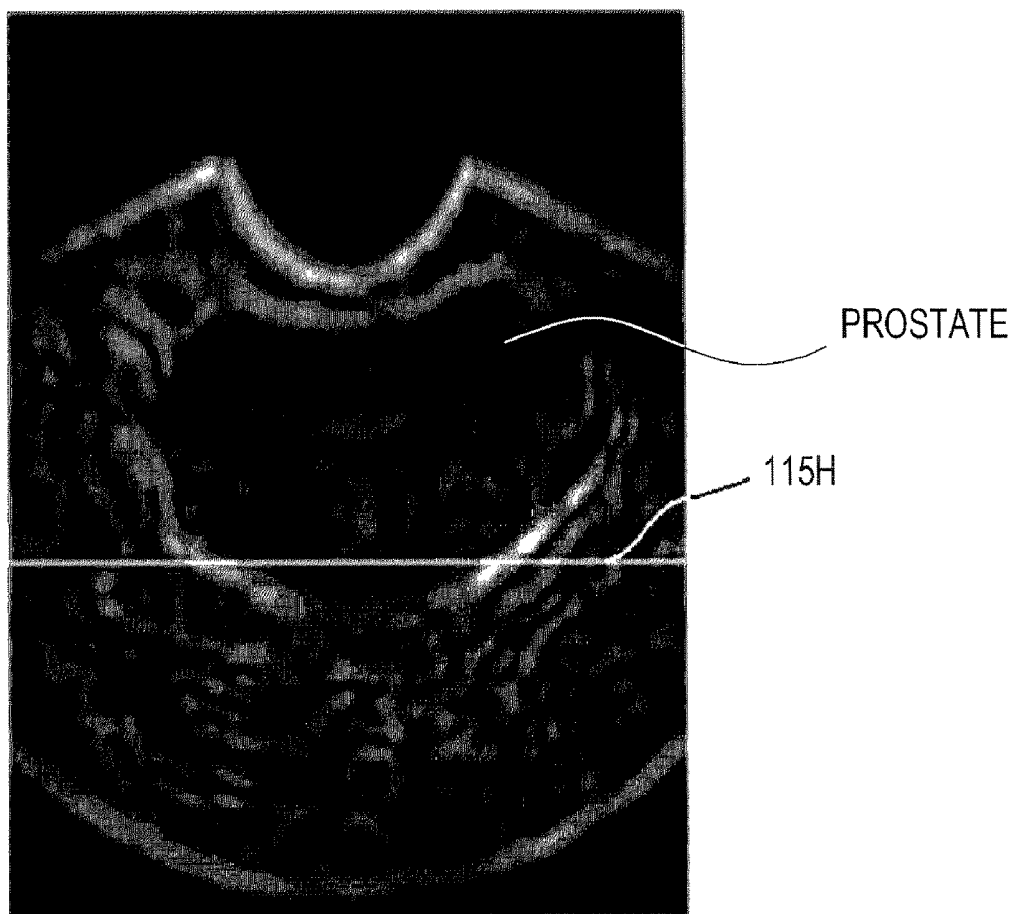


FIG. 7B

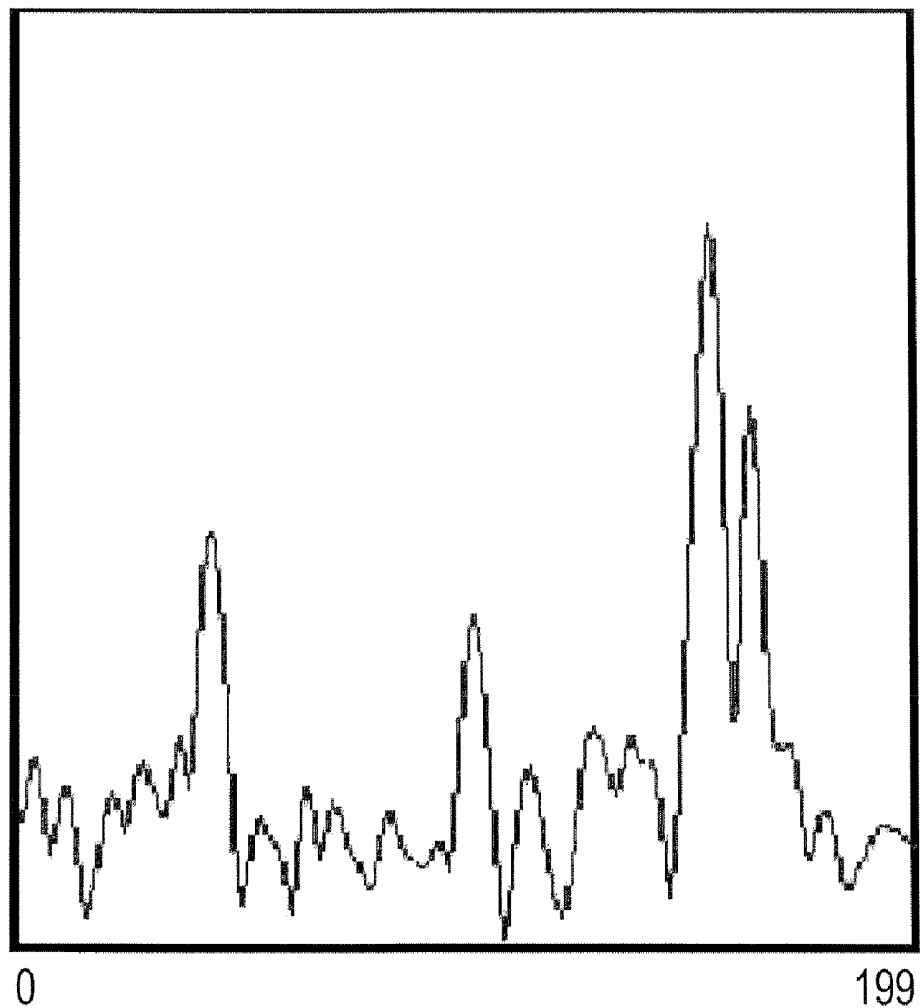


FIG. 8A

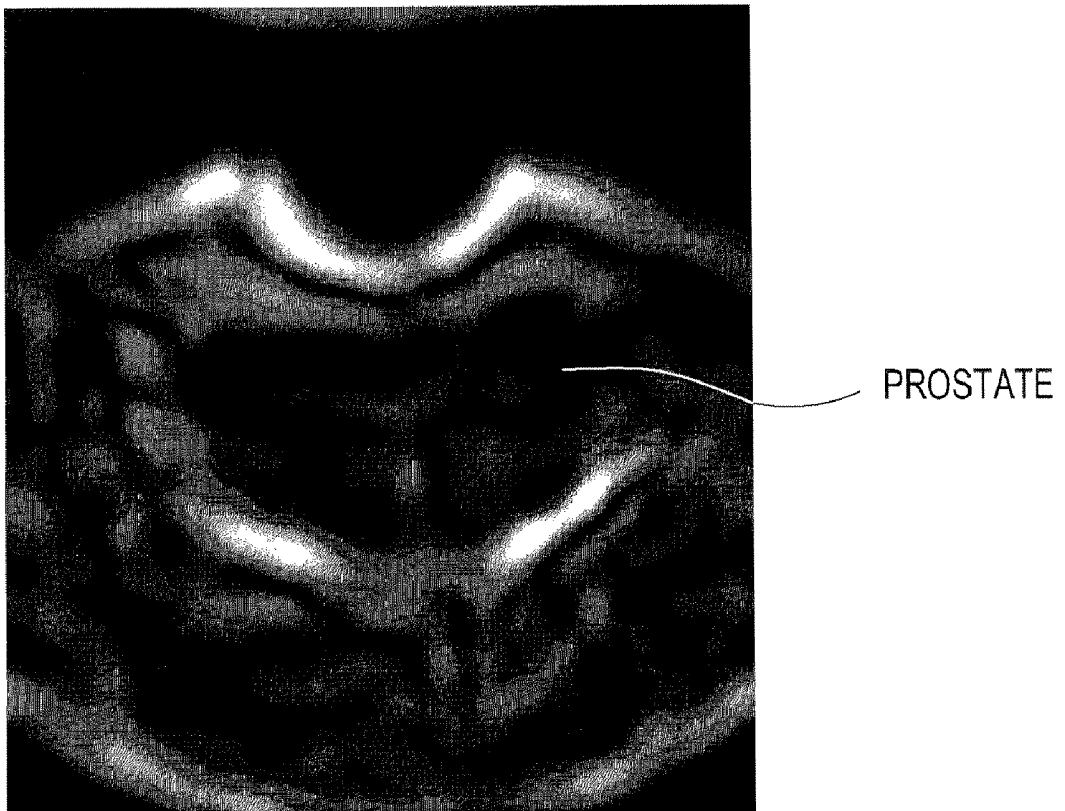


FIG. 8B

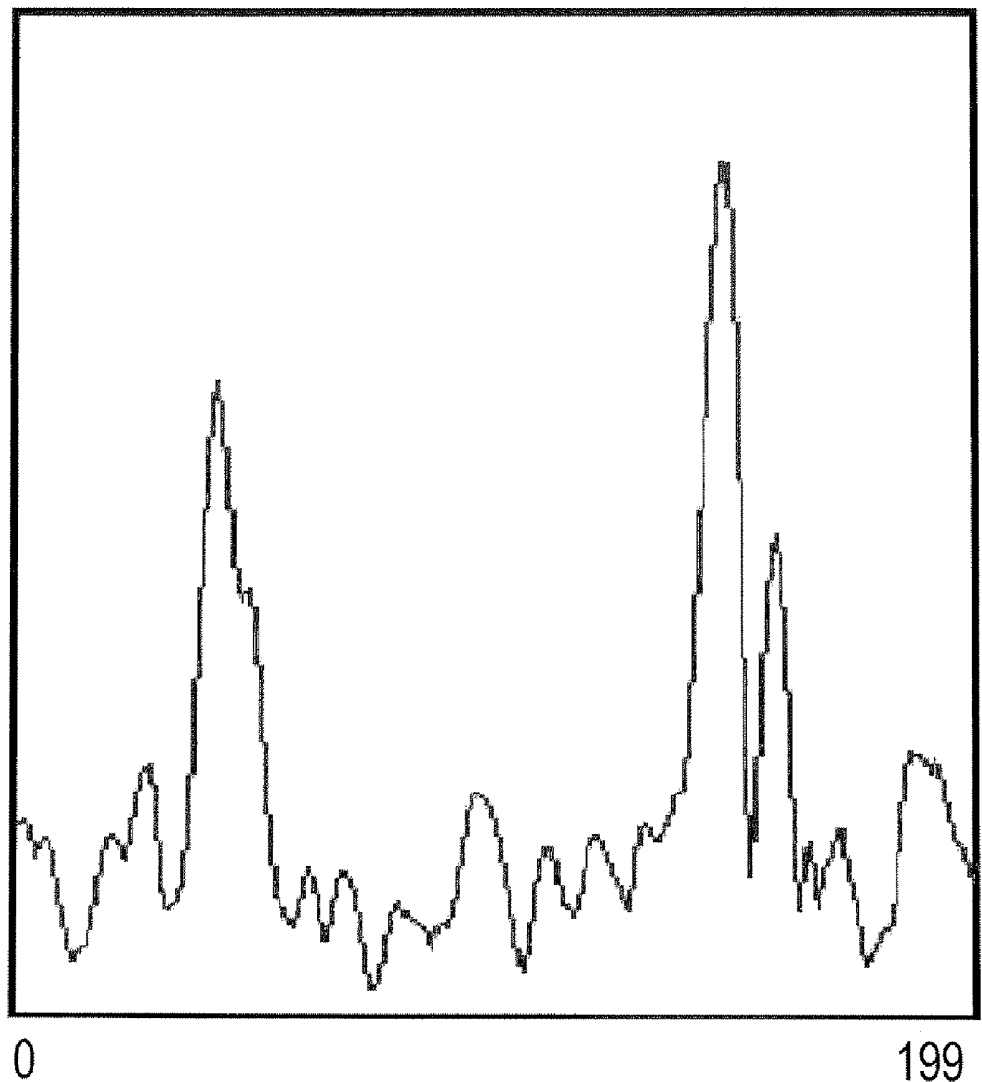


FIG. 9

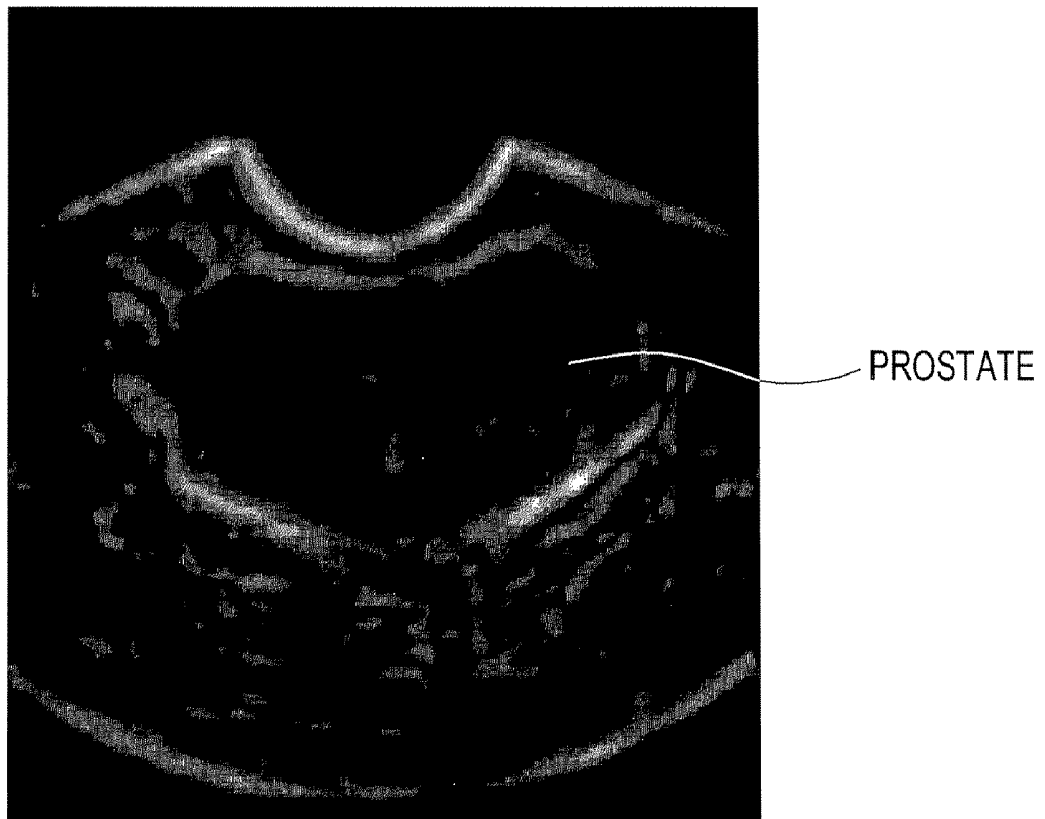


FIG. 10

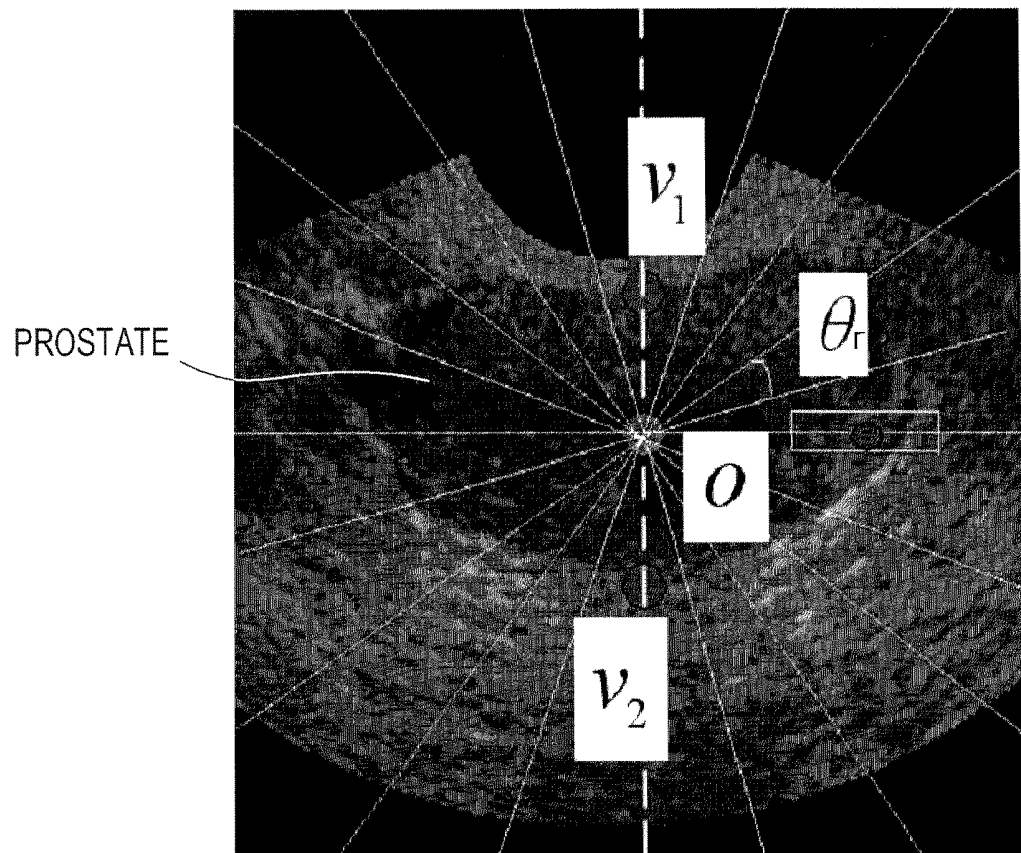


FIG. 11A

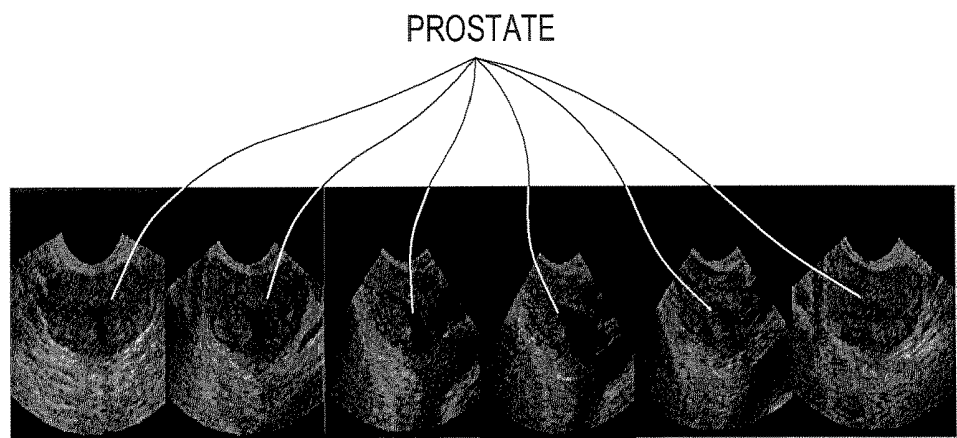


FIG. 11B

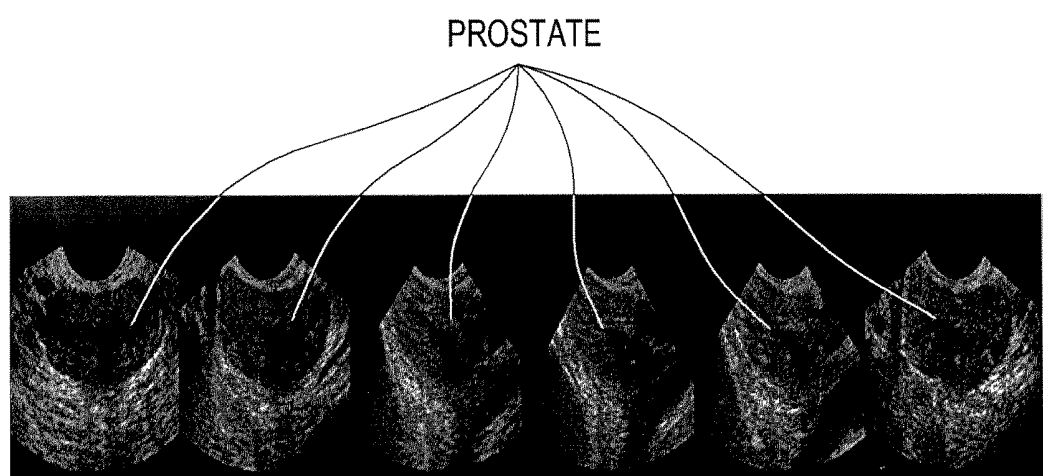


FIG. 11C

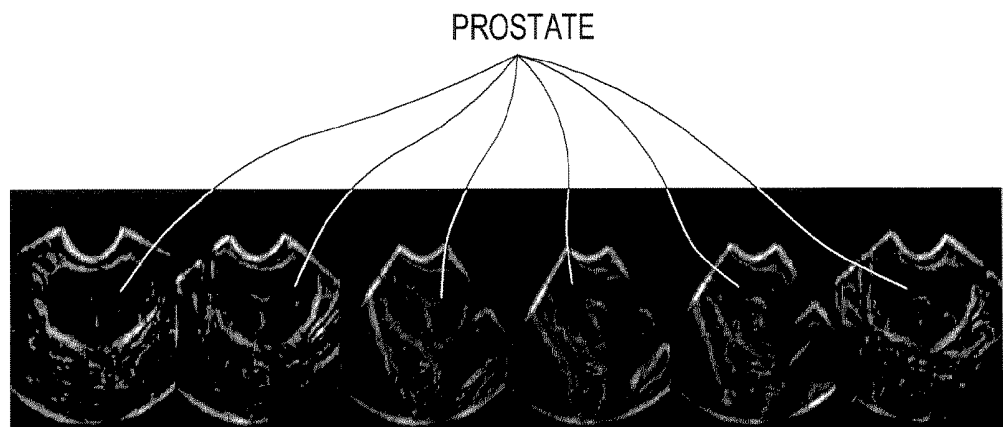


FIG. 11D

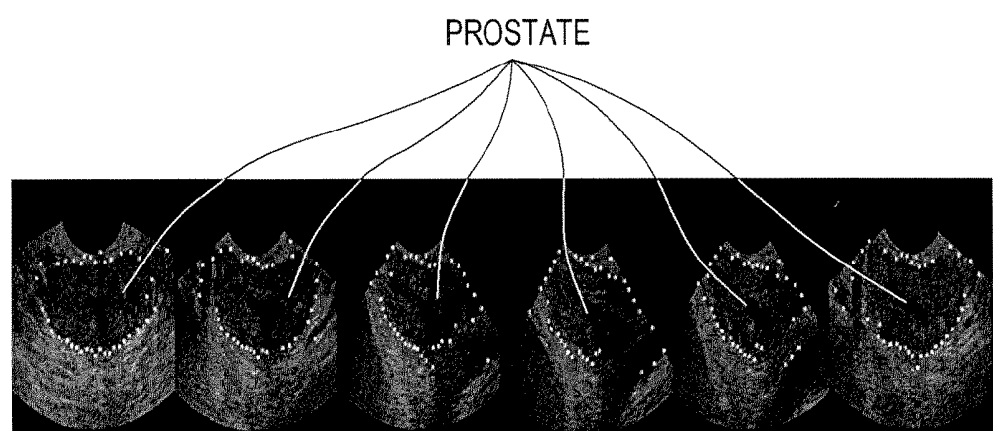


FIG. 11E

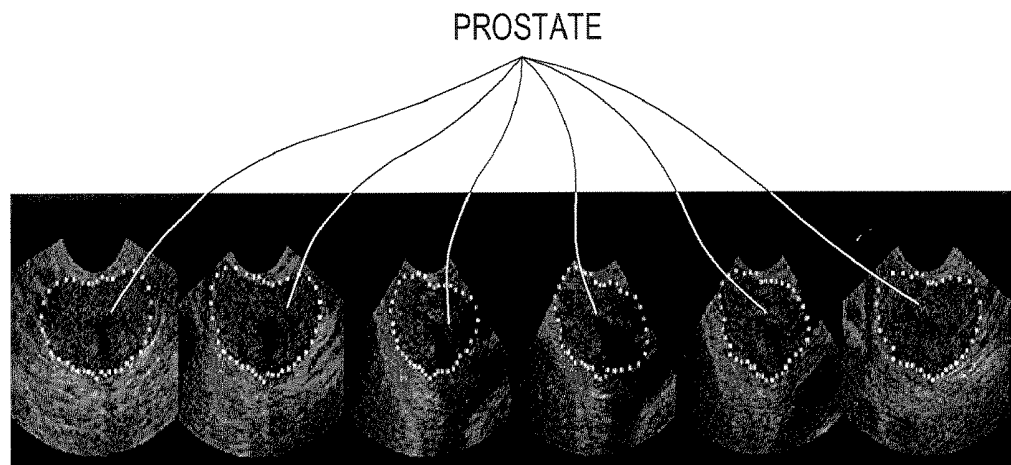
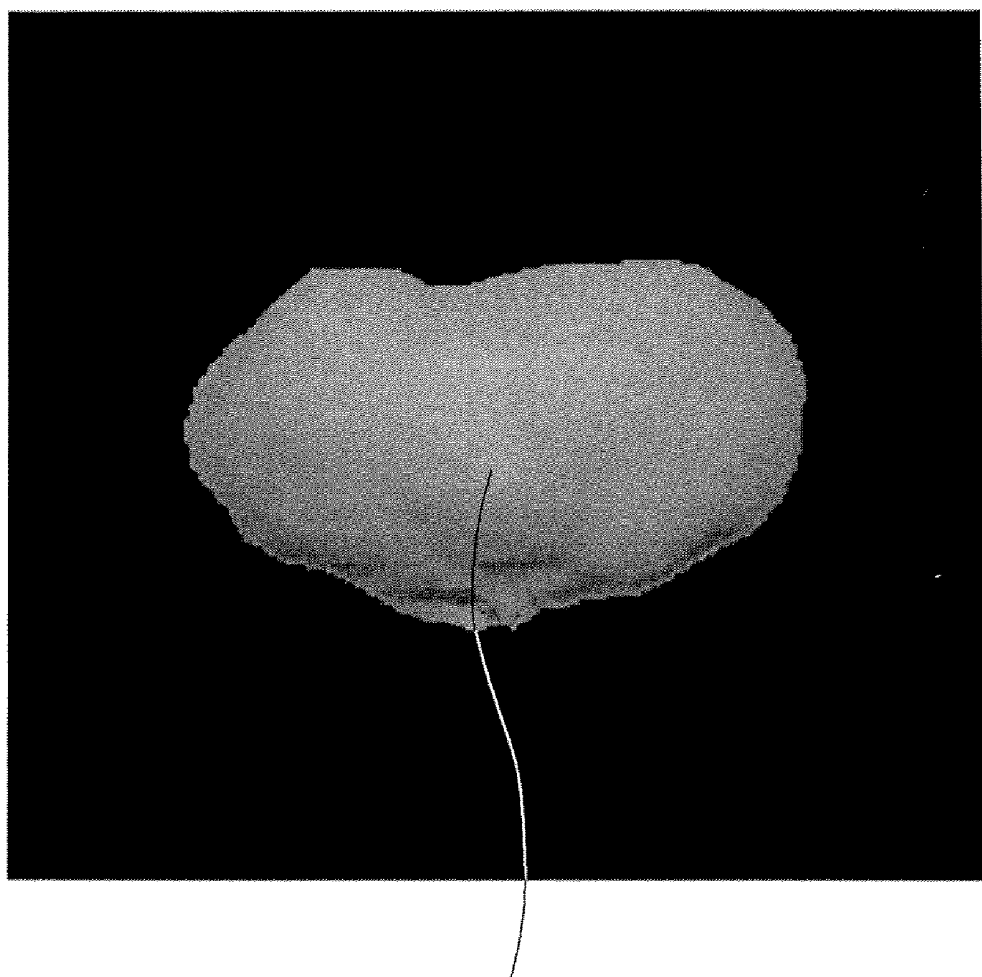
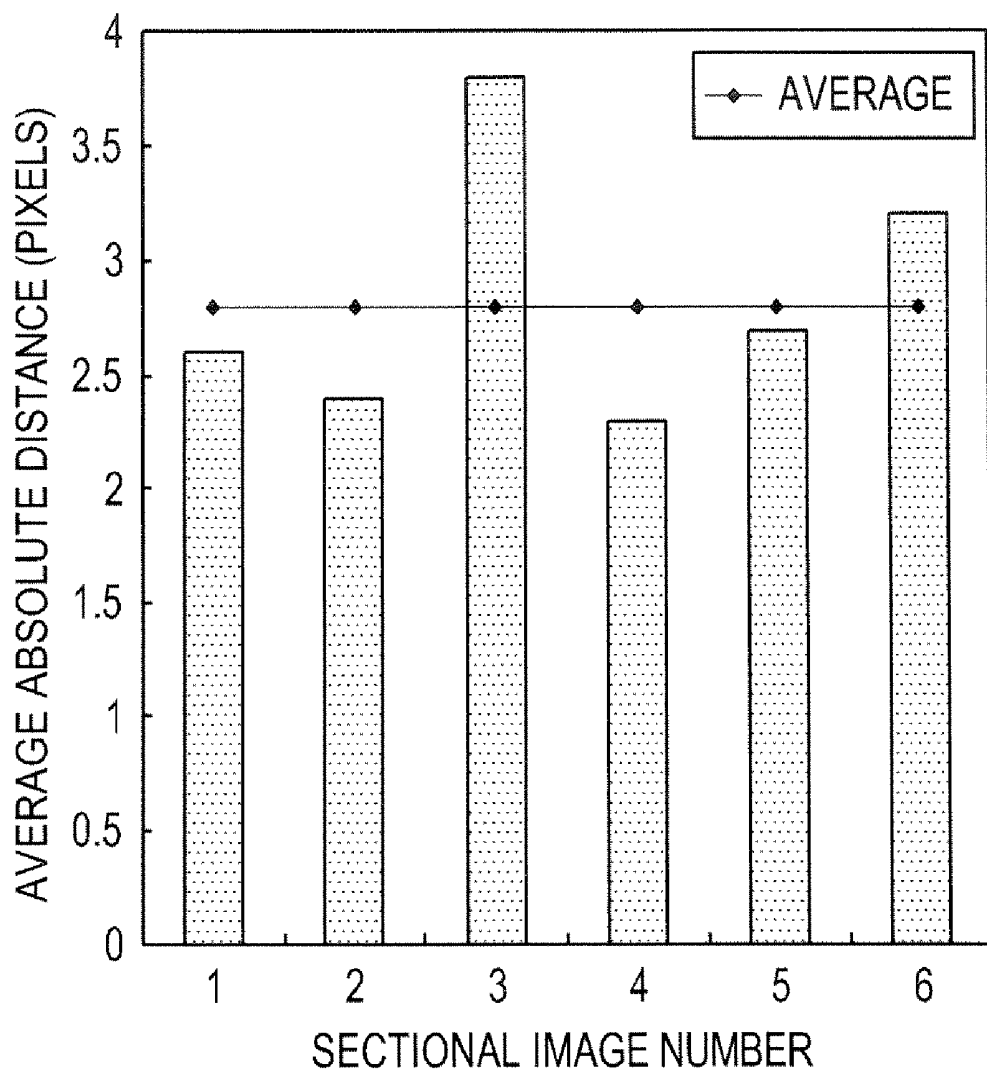


FIG. 11F



PROSTATE

FIG. 12



## ULTRASOUND IMAGING SYSTEM FOR EXTRACTING VOLUME OF AN OBJECT FROM AN ULTRASOUND IMAGE AND METHOD FOR THE SAME

### FIELD OF THE INVENTION

[0001] The present invention generally relates to an ultrasound imaging system and a method for processing an ultrasound image, and more particularly to an ultrasound imaging system for automatically extracting volume data of a prostate and a method for the same.

### BACKGROUND OF THE INVENTION

[0002] An ultrasound diagnostic system has become an important and popular diagnostic tool due to its wide range of applications. Specifically, due to its non-invasive and non-destructive nature, the ultrasound diagnostic system has been extensively used in the medical profession. Modern high-performance ultrasound diagnostic systems and techniques are commonly used to produce two or three-dimensional (2D or 3D) diagnostic images of a target object. The ultrasound diagnostic system generally uses a wide bandwidth transducer to transmit and receive ultrasound signals. The ultrasound diagnostic system forms ultrasound images of the internal structures of the target object by electrically exciting the transducer to generate ultrasound pulses that travel into the target object. The ultrasound pulses produce ultrasound echoes since they are reflected from a discontinuous surface of acoustic impedance of the internal structure, which appears as discontinuities to the propagating ultrasound pulses. The various ultrasound echoes return to the transducer and are converted into electrical signals, which are amplified and processed to produce ultrasound data for an image of the internal structure.

[0003] A prostate is a chestnut-sized exocrine gland in a male and located just below a bladder. An ejaculation duct and a urethra pass through a center of the prostate. Thus, if the prostate is inflamed or enlarged, it can cause various urinary problems. Prostate-related diseases can often occur in men over 60 years old. In the U.S., prostate cancer is the second leading cause of cancer death in men. It is predicted that the number of prostate patients will increase in the future since more men are becoming older these days. However, if discovered early, the prostate cancer can be treated. Thus, the early diagnosis is very important.

[0004] The ultrasound diagnostic system is widely employed for the early diagnosis and treatment of the prostate cancer due to its lower cost, portability, real-time imaging and the like. Mostly, a contour of the prostate is manually extracted from cross-sectional images of the prostate displayed on the screen of the ultrasound diagnostic system to thereby obtain volume information of the prostate. In such a case, it takes a long time to extract the prostate contour. Further, different extraction results are obtained when one user repeatedly extracts contours from the same sectional image or when different users extract contours from the same sectional image.

[0005] Recently, methods for automatically or semi-automatically extracting the prostate contour from the ultrasound images have been studied extensively.

[0006] Hereinafter, a conventional method for extracting the prostate contour from the ultrasound sectional images using wavelet transform and snakes algorithm will be described.

[0007] First, images are obtained at respective scales by a wavelet transform, wherein an image is repeatedly filtered with a low-pass filter and a high-pass filter horizontally and vertically. Among those images, an image obtained at a specific scale, in which prostate contour is distinguished from speckle noises, is employed to manually draw a first draft contour of the prostate thereon.

[0008] Next, on an image obtained at the scale (one step lower than the specific scale), the more accurate contour of the prostate is detected by using the snakes algorithm based on the first draft contour. By repeating this down to the lowest scale, the prostate contour can be more accurately detected step by step.

[0009] The above-mentioned conventional method has merits in that speckle noises can be reduced in the low-pass image obtained by the wavelet transform and the accuracy of the contour can be assured by using relationship between wavelet coefficients in different bands. On the other hand, the conventional method is disadvantageous in that the user has to manually draw draft contours on all the 2D cross-sectional images obtained from the 3D volume in the snakes algorithm and the contour detection results considerably depend on snakes variables.

[0010] On the other hand, there has been proposed another method for extracting the prostate contour from the ultrasound cross-sectional images by manually connecting edges extracted therefrom.

[0011] In such a method, the ultrasound cross-sectional images are first filtered with a stick-shaped filter and an anisotropic diffusion filter to reduce speckle noises.

[0012] Next, edges are automatically extracted from the images based on pre-input information such as the shape of the prostate and echo patterns. Then, the user manually draws the prostate contour based on the extracted edges. According to such a method, substantially accurate and consistent results can be obtained regardless of the users. However, the time required for extracting the prostate contour can still be long depending on the sizes of input images and the stick-shaped filter. Thus, the user has to intervene in drawing the prostate contour on all ultrasound cross-sectional images.

### SUMMARY OF THE INVENTION

[0013] The present invention provides an ultrasound imaging system for automatically extracting volume data of a prostate with wavelet transformation and a support vector machine and a method for the same.

[0014] In accordance with one aspect of the present invention, there is provided an ultrasound imaging system for forming 3D volume data of a target object, which includes: a three-dimensional (3D) image providing unit for providing a 3D ultrasound image; a pre-processing unit for forming a number of two-dimensional (2D) images from the 3D ultrasound image and normalizing the 2D images, respectively, to form normalized 2D images; an edge extraction unit for forming wavelet-transformed images of the normalized 2D images at a number of scales, forming edge images by averaging the wavelet-transformed images at a number of scales, and thresholding the edge images; a control point determining unit for determining control points by using a support vector machine (SVM) based on the normalized 2D

images, the wavelet-transformed images and the thresholded edge images; and a rendering unit for forming 3D volume data of the target object by 3D rendering based on the control points.

[0015] In accordance with another aspect of the present invention, there is provided a method for extracting 3D volume data of a target object, which includes: forming a number of two-dimensional (2D) images from a three-dimensional (3D) image; normalizing the 2D images to create normalized 2D images, respectively; forming wavelet-transformed images of the normalized 2D images at a number of scales; forming edge images by averaging the wavelet-transformed images at a number of scales; thresholding the edge images; determining control points by using a support vector machine (SVM) based on the normalized 2D images, the wavelet-transformed images and the thresholded edge images; and forming 3D volume data of the target object by 3D rendering based on the control points.

[0016] In accordance with the present invention, there are provided an ultrasound imaging system and method for extracting volume data of an object from 3D ultrasound image data by using wavelet transform and SVM. Thus, it is possible to obtain a clear contour of the object while reducing noises in the edge image formed by averaging wavelet-transformed images at respective scales.

#### BRIEF DESCRIPTION OF THE DRAWINGS

[0017] The above and other objects and features of the present invention will become apparent from the following description of an embodiment given in conjunction with the accompanying drawings, in which:

[0018] FIG. 1 is a block diagram showing an ultrasound imaging system constructed in accordance with one embodiment of the present invention;

[0019] FIG. 2 is a diagram for explaining acquisition of 2D cross-sectional images from 3D image;

[0020] FIGS. 3A and 3B are ultrasound pictures showing 2D cross-sectional images obtained from different volumes;

[0021] FIGS. 4A and 4B are ultrasound pictures obtained by normalizing the pixel values of the 2D cross-sectional images shown in FIGS. 3A and 3B;

[0022] FIG. 5 is an exemplary diagram showing a wavelet transform process;

[0023] FIG. 6A is an ultrasound picture showing a pre-processed prostate image;

[0024] FIGS. 6B to 6D are ultrasound pictures showing images at scales  $2^2$ ,  $2^3$  and  $2^4$  obtained by performing wavelet transform on the pre-processed prostate image;

[0025] FIG. 7A shows a wavelet-transformed image at scale  $2^3$ ;

[0026] FIG. 7B shows a waveform in the 115<sup>th</sup> horizontal line in the wavelet-transformed image shown in FIG. 7A;

[0027] FIG. 8A shows an edge image obtained by averaging wavelet-transformed images at scales  $2^2$ ,  $2^3$  and  $2^4$ ;

[0028] FIG. 8B shows a waveform in the 115<sup>th</sup> horizontal line in the edge image shown in FIG. 8A;

[0029] FIG. 9 is an ultrasound picture showing a thresholded edge image;

[0030] FIG. 10 shows radial lines arranged around a center of the prostate;

[0031] FIGS. 11A to 11F show images obtained by a method for extracting a 3D ultrasound prostate volume in accordance with one embodiment of the present invention; and

[0032] FIG. 12 is a graph showing average absolute distances for cross-sectional images.

#### DETAILED DESCRIPTION OF THE PRESENT INVENTION

[0033] Hereinafter, an ultrasound imaging system and method for automatically extracting a volume of a target object (for example, a prostate) in accordance with the present invention will be described with reference to the accompanying drawings.

[0034] Referring now to FIG. 1, an ultrasound imaging system 100 for forming volume data of a target object in accordance with one embodiment of the present invention includes a 3D ultrasound image providing unit 10, a pre-processing unit 20, an edge extraction unit 30, a control point determining unit 40 and a 3D rendering unit 50. The 3D image providing unit 10 can be a memory or a probe. The pre-processing unit 20, the edge extraction unit 30, the control point determining unit 40 and the 3D rendering unit 50 can be embodied with one processor. The control point determining unit 40 includes a support vector machine (SVM).

[0035] Here, an edge is a point where the discontinuity of brightness appears. Further, a boundary is a contour of the target object, for example, a prostate.

##### 1. Pre-processing

[0037] A method for acquiring 2D cross-sectional images from the 3D image will be described with reference to FIG. 2. In FIG. 2, a rotation axis RX is a virtual axis passing through a center of the 3D image VD provided with unit 10. The pre-processing unit 20 produces a number of the 2D cross-sectional images by rotating the 3D image by specified angles  $\theta$  around the rotation axis RX. In this embodiment, six 2D cross-sectional images with an image size of 200×200 are produced at every 30 degrees around the rotation axis RX.

[0038] Next, the average and standard deviation of a pixel value (preferably, brightness and contrast) of each 2D cross-sectional image are normalized. At this time, a background having brightness of zero in the 2D ultrasound image is excluded from normalization. In this embodiment, the average and standard deviation are set to be 70 and 40, respectively.

[0039] FIGS. 3A and 3B are ultrasound pictures showing 2D cross-sectional images obtained from different 3D images. FIGS. 4A and 4B are ultrasound pictures obtained by normalizing the 2D cross-sectional images shown in FIGS. 3A and 3B. As shown in FIGS. 4A and 4B, normalization yields images having uniform brightness characteristics regardless of 3D input images.

## [0040] 2. Edge Extraction

[0041] The edge extraction unit **30** decomposes the 2D cross-sectional image into a set of sub-band images. Namely, the edge extraction unit **30** applies the wavelet decomposition to the normalized 2D cross-sectional images provided from the pre-processing unit **20** in the manner shown in FIG. 5 by using Equations 1 to 3.

$$W_2^H f(m,n) = S_{2^{j-1}} f(m,n) * g(m/2^{j-1}) * \delta(n) \quad \text{Eq. 1}$$

$$W_2^V f(m,n) = S_{2^{j-1}} f(m,n) * \delta(m) * g(n/2^{j-1}) \quad \text{Eq. 2}$$

$$S_2 f(m,n) = S_{2^{j-1}} f(m,n) * h(m/2^{j-1}) * h(n/2^{j-1}) \quad \text{Eq. 3}$$

[0042] In Equations 1 to 3,  $f(m,n)$  represents a pre-processed image;  $h(n)$  and  $g(n)$  respectively represent a low-pass filter and a high-pass filter for wavelet transform; and  $\delta(x)$  represents an impulse function. The superscripts  $H$  and  $V$  denote horizontal and vertical filtering, respectively. Further,  $W_2^H f(m,n)$  and  $W_2^V f(m,n)$  respectively represent high-pass images containing vertical and horizontal edge information at scale  $2^j$ , whereas  $S_2 f(m,n)$  represents a low-pass image at scale  $2^j$  obtained from the pre-processed image  $f(m,n)$ . The pre-processed image  $f(m,n)$  can be represented as  $S_2 f(m,n)$ .

[0043] Next, the results of the wavelet transform at scale  $2^j$  are applied to Equation 4 to obtain images  $M_2 f(m,n)$  at scale  $2^j$ .

$$M_2 f(x,y) = \sqrt{|W_2^H f(m,n)|^2 + |W_2^V f(m,n)|^2} \quad \text{Eq. 4}$$

[0044] FIG. 6A shows a pre-processed prostate image and FIGS. 6B to 6D respectively show wavelet-transformed images  $M_2 f(m,n)$ ,  $M_2^3 f(m,n)$  and  $M_2^4 f(m,n)$  at scales  $2^2$ ,  $2^3$  and  $2^4$  obtained by performing wavelet transform on the pre-processed prostate image. As shown in FIGS. 6B to 6D, the prostate and noises can be apparently discriminated as the scale is increased. However, the boundary of the prostate becomes too unclear to accurately capture a position of the boundary.

[0045] Then, in order to reduce noises in the image and clear the boundary of the prostate, wavelet-transformed images at each scale are averaged by using Equation 5.

$$Mf(m, n) = \frac{1}{3} \sum_{j=2}^4 \frac{M_2 j f(m - d_{2j}, n - d_{2j})}{\max_{(m,n)}(M_2 j f(m - d_{2j}, n - d_{2j}))} \quad \text{EQ. 5}$$

[0046] In Equation 5,

$$\max_{(m,n)}(\cdot)$$

is an operator for computing a maximum pixel value in images, and  $Mf(m,n)$  represents an edge image obtained by averaging the wavelet-transformed images. On the other hand, since the centers of the filters are delayed by  $1/2$  in Equations 1 to 3, the images at the respective scales are horizontally and vertically compensated by

$$d_{2j} = (1/2) \cdot \sum_{n=1}^j 2^{n-1}$$

before averaging, so that the boundary positions of the prostate can be set to be equal regardless of scales. FIGS. 7A, 7B, 8A and 8B show effects obtained when wavelet-transformed images are averaged. FIG. 7A shows the wavelet-transformed image at scale  $2^3$ , whereas FIG. 7B shows a waveform of the 115<sup>th</sup> horizontal line in the image shown in FIG. 7A. FIG. 8A shows an edge image obtained by averaging wavelet-transformed images at scales  $2^2$ ,  $2^3$  and  $2^4$ , whereas FIG. 8B shows a waveform of the 115<sup>th</sup> horizontal line in the edge image shown in FIG. 8A. By comparing FIGS. 7A and 8A, it can be seen that the edge image (FIG. 8A) obtained by averaging shows less noises and a clearer boundary than the image (FIG. 7A), which has only undergone the wavelet transformation.

[0047] Next, in order to reduce noises in the edge image obtained by averaging, the brightness of the edge image is thresholded with Equation 6.

$$M_T f(m, n) = \begin{cases} Mf(m, n) & \text{if } Mf(m, n) > Th \\ 0 & \text{otherwise} \end{cases} \quad \text{Eq. 6}$$

[0048] In Equation 6,  $Th$  represents the threshold, and  $M_T f(m,n)$  represents a thresholded edge image obtained from the edge image  $Mf(m,n)$ . FIG. 9 shows the thresholded edge image.

[0049] In short, an edge image with less speckle noises can be obtained by the above-mentioned edge extraction, wherein images at respective scales obtained by performing wavelet transform on a 2D cross-sectional image are averaged to form an edge image and the edge image is then thresholded.

## [0050] 3. Determining of Control Points

[0051] Control points are determined based on the fact that an inner portion of the prostate is darker than an external portion thereof in the ultrasound image. The control points will be used to obtain the prostate volume through 3D rendering. The control point determining unit **40** is provided with the thresholded edge image  $M_T f(m,n)$  and the wavelet-transformed images from the edge extraction unit **30**. Such a unit then determines a number of control points at which the prostate contour intersects predetermined directional lines, preferably, radial lines in the pre-processed image  $f(m,n)$ . FIG. 10 shows the radial lines arranged around a center point  $O$  of the prostate, from which the radial lines are originated. The center point  $O$  is determined with a midpoint between two reference points  $v_1$  and  $v_2$  selected by the user. Hereinafter, a method of determining the control points will be described in detail.

[0052] The control point determining unit **40** searches first candidate points having brightness greater than zero along the radial lines, respectively with the thresholded edge image  $M_T f(m,n)$ .

[0053] Next, internal and external windows having a size of  $M \times N$  are set around each of the first candidate points in a low-pass sub-band image at a predetermined scale, produced by the wavelet transform. The internal and external windows are adjacent each other over the first candidate point. Then, by comparing averages of the brightness of the internal and external windows, the first candidate points of which the external window has greater average brightness than the internal window are set as second candidate points. In this embodiment, the second candidate points are selected by using the wavelet-transformed low-pass sub-band image  $S_2 f(m,n)$  at scale  $2^3$ .

[0054] Next, feature vectors at the second candidate points are generated by using a support vector machine (SVM) in order to classify the second candidate points into two groups of points, wherein one group of points have characteristics of the control points and the other group of points do not. For this, first, internal and external windows having a size of  $M \times N$  are set around each of the second candidate points along a radial direction on the pre-processed image  $f(m,n)$ . Then, averages and standard deviations of the windows in the pre-processed image, block difference invert probabilities (BDIP), averages of block variation of local correlation coefficients (BVLC) are obtained to generate the feature vectors expressed by the following Equation 7.

$$h = \begin{bmatrix} \mu_{\text{out}}(f), \mu_{\text{in}}(f), \sigma_{\text{out}}(f), \sigma_{\text{in}}(f), \mu_{\text{out}}(D), \mu_{\text{in}}(D), \mu_{\text{out}}(V), \\ \mu_{\text{in}}(V) \end{bmatrix} \quad \text{Eq. 7}$$

[0055] In Equation 7,  $\mu_{\text{out}(\text{in})}(\cdot)$  and  $\sigma_{\text{out}(\text{in})}(\cdot)$  respectively represent the average and standard deviation in the external (internal) window, and D and V denote BDIP and BVLC, respectively, for the pre-processed image.

[0056] BDIP is defined as a ratio of a sum of values, which are obtained by subtracting the pixel values in the block from the maximum pixel value in the block, to the maximum pixel value in the block. The BVLC is defined with a difference between the maximum and the minimum correlation coefficients among four local correlation coefficients at one pixel in a block. The BDIP and BVLC are well-known and, thus, detailed description thereof will be omitted herein.

[0057] After obtaining the feature vectors of all the second candidate points as described above, in order to prevent specified components of the feature vectors from affecting SVM classification, respective components of the feature vectors are normalized as Equation 8.

$$x = h/\sigma \quad \text{Eq. 8}$$

[0058] In Equation 8, “/” denotes component-wise division of two vectors;  $\sigma$  is a vector defined with a standard deviation calculated from the columns of the respective components of  $h$ ; and  $x$  is a normalized feature vector.

[0059] Next, the most appropriate point for the control points among the second candidate points is determined in each radial direction by using a trained SVM based on the brightness in the thresholded edge image  $M_T f(m,n)$ . Then, the detected points are determined to be third candidate points in respective radial directions. If all the second candidate points in a specified radial direction are determined not to be appropriate for the control points, a brightest point among the second candidate points of the radial direction in the edge image is selected as the third candidate point.

[0060] On the other hand, data used for training the SVM contain points divided into two groups, wherein one group including the points, artificially determined by the user and has characteristics of the control points, and the other group including the points that do not meet the characteristics of the control point. The feature vectors are extracted from the points of the two groups by using Equation 8 to train the SVM. In this embodiment, to train the SVM, 60 points with characteristics of the control points and 60 points with no characteristics of the control points are extracted from images unrelated to the prostate. Further, windows set in the images for extracting the feature vectors have a size of  $9 \times 3$ .

[0061] Then, while taking a basic contour of the target object into account, that is, supposing that the contour of the prostate curves gently, the positions of the third candidate points are readjusted as expressed by Equation 9.

$$\hat{P}_i = \frac{P_{i-1} + P_{i+1}}{2}, \text{ if } |P_i - P_{i-1}| > \frac{1}{N} \sum_{i=1}^N |P_i - P_{i-1}| \quad \text{Eq. 9}$$

[0062] In Equation 9,  $P_i$  represents the positions of the third candidate points in the  $i^{\text{th}}$  radial line.

[0063] Then, points corresponding to the edges of the greatest brightness within specified ranges, which include the readjusted third candidate points, are finally determined as the control points in the respective radial directions.

[0064] The 3D rendering unit 50 constructs a 3D wire frame of a polyhedron object (i.e., the prostate) based on the determined control points to obtain an ultrasound prostate volume by using surface-based rendering techniques.

[0065] FIGS. 11A to 11F show images obtained at each step in a method for extracting a 3D ultrasound prostate volume in accordance with the present invention. FIG. 11A shows the 2D cross-sectional images obtained at every 30 degrees by rotating the 3D image. FIG. 11B shows the images obtained by normalizing the brightness of the images shown in FIG. 11A. By comparing FIGS. 11A and 11B, it can be seen that the brightness normalized images (FIG. 11B) show clearer boundaries than FIG. 11A. FIG. 11C shows images configured with the thresholded edge image  $M_T f(m,n)$ , which was obtained by averaging and thresholding images  $\{M_j f(m,n)\}$  ( $2 \leq j \leq 4$ ). FIG. 11D shows the third candidate points determined by the SVM. FIG. 11E shows images containing the readjusted third candidate points, which have gentle contours compared to those in FIG. 11D. Finally, FIG. 11F shows the 3D prostate volume extracted from the ultrasound image based on the control points by using the surface-based rendering techniques.

[0066] The performance of the 3D prostate volume extraction in accordance with the present invention can be evaluated by using an average absolute distance defined as Equation 10.

$$e_M = \frac{1}{N} \sum_{i=0}^{N-1} \min_j |b_j - a_i| \quad \text{Eq. 10}$$

**[0067]** In Equation 10,  $e_M$  represents average absolute distances;  $a_i$  represents control points on the contour  $A=\{a_0, a_1, \dots, a_{N-1}\}$  that is extracted manually, and  $b_j$  represents control points on the contour  $B=\{b_0, b_1, \dots, b_{N-1}\}$  that is obtained by using the above-mentioned method. FIG. 12 shows the average absolute distances  $e_M$  for cross-sectional images. Referring to FIG. 12, the average absolute distances  $e_M$  range from about 2.3 to 3.8 pixels and average 2.8 pixels. It exhibits a similar performance as the conventional method of manually extracting the contour, in which  $e_M$  is about 2 pixels on the average.

**[0068]** In the ultrasound imaging system and method of the present invention, the volume of the prostate is extracted from the 3D ultrasound image with the wavelet transformation and the SVM. The wavelet-transformed images at same scale are averaged to reduce noise and to obtain apparent boundary of the object on the edge image.

**[0069]** While the present invention has been described and illustrated with respect to an embodiment of the invention, it will be apparent to those skilled in the art that variations and modifications are possible without deviating from the broad principles and teachings of the present invention which should be limited solely by the scope of the claims appended hereto.

What is claimed is:

**1.** An ultrasound imaging system for forming 3D volume data of a target object, comprising:

a three-dimensional (3D) image providing unit for providing a 3D ultrasound image;

a pre-processing unit adapted to form a number of two-dimensional (2D) images from the 3D ultrasound image and normalize the 2D images to form normalized 2D images;

an edge extraction unit adapted to form wavelet-transformed images of the normalized 2D images at a number of scales, the edge extraction unit further being adapted to form edge images by averaging the wavelet-transformed images at a number of scales and threshold the edge images;

a control point determining unit adapted to determine control points by using a support vector machine (SVM) based on the normalized 2D images, the wavelet-transformed images and the thresholded edge images; and

a rendering unit adapted to form 3D volume data of the target object by 3D rendering based on the control points.

**2.** The ultrasound imaging system of claim 1, wherein the target object is a prostate.

**3.** The ultrasound imaging system of claim 1, wherein the pre-processing unit normalizes an average and a standard deviation of said 2D images to form the normalized 2D images.

**4.** The ultrasound imaging system of claim 3, wherein the rendering unit renders at least one of the normalized 2D images, the wavelet-transformed images and the thresholded edge images based on the control points.

**5.** The ultrasound imaging system of claim 3, wherein the control point determining unit determines the control points by:

arranging a plurality of radial lines around a center of the target object in the thresholded edge images;

selecting first candidate points with a brightness greater than zero on each of the radial lines;

setting internal and external windows around each of the first candidate points;

comparing averages of the brightness in internal and external windows in the wavelet-transformed image at a predetermined scale;

selecting second candidate points with a greater brightness average in the external window than in the internal window among the first candidate points on each of the radial lines;

generating feature vectors of the second candidate points in the normalized 2D image and normalizing components of the feature vectors;

training the SVM by using the normalized feature vectors;

selecting third candidate points with the greatest brightness among the second candidate points on each of the radial lines in the thresholded edge images by using the trained SVM;

readjusting positions of the third candidate points based on a basic contour of the target object; and

determining an edge part of the target object with the greatest brightness within a predetermined distance among the readjusted third candidate points as the control points.

**6.** A method for extracting 3D volume data of a target object, comprising:

forming a number of two-dimensional (2D) images from a three-dimensional (3D) image;

normalizing the 2D images to create normalized 2D images;

forming wavelet-transformed images of the normalized 2D images at a number of scales;

forming edge images by averaging the wavelet-transformed images at a number of scales;

thresholding the edge images;

determining control points by using a support vector machine (SVM) based on the normalized 2D images, the wavelet-transformed images and the thresholded edge images; and

forming 3D volume data of the target object by 3D rendering based on the control points.

**7.** The method of claim 6, wherein the target object is a prostate.

**8.** The method of claim 6, wherein normalizing the 2D images includes normalizing an average and a deviation of brightness in the 2D images.

**9.** The method of claim 8, wherein the 3D volume data is formed by rendering at least one of the normalized 2D images, the wavelet-transformed images and the thresholded edge images based on the control points.

**10.** The method of claim 9, wherein determining the control points includes:

arranging a plurality of radial lines around a center of the target object in the thresholded edge images;

selecting first candidate points with a brightness greater than zero on each of the radial lines;

setting internal and external windows around each of the first candidate points;

comparing averages of the brightness in internal and external windows in the wavelet-transformed image at a predetermined scale;

selecting second candidate points with a greater brightness average in the external window than in the internal window among the first candidate points on each of the radial lines;

generating feature vectors of the second candidate points in the normalized 2D image and normalizing components of the feature vectors;

training the SVM by using the normalized feature vectors;

selecting third candidate points with the greatest brightness among the second candidate points on each of the radial lines in the thresholded edge image by using the trained SVM;

readjusting positions of the third candidate points based on a basic contour of the target object; and

determining an edge part of the target object with the greatest brightness within a predetermined distance among the readjusted third candidate points as the control points.

\* \* \* \* \*

专利名称(译)	用于从超声图像中提取物体的体积的超声成像系统及其方法		
公开(公告)号	<a href="#">US20070167779A1</a>	公开(公告)日	2007-07-19
申请号	US11/539460	申请日	2006-10-06
申请(专利权)人(译)	MEDISON CO. , LTD.		
当前申请(专利权)人(译)	MEDISON CO. , LTD.		
[标]发明人	KIM NAM CHUL OH JONG HWAN KIM SANG HYUN KWAK JONG IN AHN CHI YOUNG		
发明人	KIM, NAM CHUL OH, JONG HWAN KIM, SANG HYUN KWAK, JONG IN AHN, CHI YOUNG		
IPC分类号	A61B8/00		
CPC分类号	A61B8/08 A61B8/483 G06K9/4609 G06K9/4671 G06K9/6254 G06T2207/30081 G06T7/0083 G06T7/0095 G06T2207/10132 G06T2207/20064 G06K2209/05 G06T7/12 G06T7/168		
优先权	1020050094318 2005-10-07 KR		
外部链接	<a href="#">Espacenet</a> <a href="#">USPTO</a>		

## 摘要(译)

本发明提供一种用于形成目标对象的3D体数据的超声成像系统，包括用于提供3D超声图像的三维(3D)图像提供单元;预处理单元，用于从3D超声图像形成多个二维(2D)图像，并对2D图像进行归一化以形成归一化的2D图像;边缘提取单元，用于以多个尺度形成归一化2D图像的小波变换图像，边缘提取单元还被配置为通过对多个尺度的小波变换图像进行平均并对边缘图像进行阈值来形成边缘图像;控制点确定单元，用于通过使用基于归一化2D图像的支持向量机(SVM)，小波变换图像和阈值边缘图像来确定控制点;以及基于控制点通过3D渲染形成目标对象的3D体数据的渲染单元。

